An analytical approach to evaluating magnetic-field closure and topological changes in FRC devices ᴱᴾ

🆔 T. Ahsan and 🆔 S. A. Cohen

COLLECTIONS

ᴱᴾ   This paper was selected as an Editor's Pick

View Online   Export Citation   CrossMark

Physics of Plasmas

Physics of Plasmas
Features in **Plasma Physics Webinars**

Register Today!

An analytical approach to evaluating magnetic-field closure and topological changes in FRC devices ⓔⓟ

🌐 View Online   ⤴ Export Citation   ⦿ CrossMark

T. Ahsan[1,2] ⓘⒹ and S. A. Cohen[2,a] ⓘⒹ

AFFILIATIONS

[1]Physics Department, Princeton University, Princeton, New Jersey 08540, USA
[2]Princeton Plasma Physics Laboratory, Princeton University, Princeton, New Jersey 08543, USA

[a]Author to whom correspondence should be addressed: scohen@pppl.gov

ABSTRACT

We describe mathematical methods based on optimizing a modified non-linear flux function (MFF) to evaluate whether odd-parity perturbations affect the local closure of magnetic field lines in field-reversed configurations. Using the MFF methodology, quantitative formulas are derived that provide the shift of the field minimum and the threshold for field-line opening, a discontinuous change in field topology.

Published under an exclusive license by AIP Publishing. https://doi.org/10.1063/5.0090163

I. INTRODUCTION

The local closure of magnetic field lines and their topology are appropriate proxies and the first step toward analyzing plasma confinement. It is well known from $\nabla \cdot \mathbf{B} = 0$ that all magnetic field lines close. However, closure of certain magnetic field lines can happen far away from the region of interest, the limited volume in which plasma must be confined. Small perturbations can dramatically alter and open up the local field structure, even for initially well-defined closed structures. The spatial scale of the closure is important to fusion plasma physics,[1,2] solar physics, and planetary plasma physics.[3]

This study, a step toward understanding plasma confinement by magnetic fields, provides a quantitative method to test the resilience of the field structure to intentional manipulation. Though perturbations may vary with time and interactions between the field and plasma may alter certain results, we discuss only time-independent perturbations, valid under the conditions we consider.

The field structure of radio-frequency-heated (RF) field-reversed configurations (FRCs) at an instant of time is our specific interest. The RF fields considered have frequencies well below the electron cyclotron and plasma frequencies and sufficiently below the ion cyclotron frequency to satisfy the time-independent assertion. The RF field is likely to have components parallel and perpendicular to the FRC's magnetic field and may be symmetric about the FRC's axial midplane, $z = 0$, where z is the major axis. This symmetric case is termed as even parity.

Anti-symmetric fields are termed as odd parity. An FRC's magnetic fields are odd parity and close around an equilibrium line.

Previous studies[4] of this question by graphic and numerical methods showed that an FRC's closed field structure was destroyed by even-parity perturbations but maintained by weak odd-parity ones. These studies gave a loose description of what is meant by "weak" and defined the term "local" to those field lines within the unperturbed FRC's approximately elliptical separatrix surface. The methodology we present provides detailed information on the perturbed field's shape, focusing on perturbations with long axial wavelengths. Some results, namely, preservation of field line closure, apply to arbitrary wavelengths.

At the heart of the analysis is the construction of a modified flux function (MFF), derived by solving non-linear differential field-line equations.

The analysis is formulated based on symmetry with respect to the $z = 0$ midplane. Notable observations from the analysis presented herein for small odd-parity perturbations are the field structure retains closure for a broad range of wavelengths, the field minimum shifts radially, and the closed field structures change shape within the separatrix. Quantitative values of these are derived. Though the derivations are strictly valid for long-wavelength perturbations, the accuracy turned out to be relatively high, and the analysis was adequate for wave-number $\sim 0.5/$(separatrix semi-major axis). Such agreement is attributed to the long-wavelength approximation being a second-order approximation of the perturbation. Generalization of the analysis to

arbitrary wavelengths remains to be done. A discontinuous change in the field structure at increased odd-parity perturbation is identified.

II. MODEL FRC AND ODD-PARITY PERTURBATION FIELDS

There are many FRC shapes considered in the literature, falling into categories such as elliptic, racetrack,[5] long-thin,[6] Grad–Shafranov,[7,8] MHD,[9] and Solov'ev.[10] All share the essential features, namely, a separatrix, two X-point spindle nulls on the major axis, and a single O-point line defining the minor axis. In this study, we restrict attention to the Solov'ev, which, being analytic, is appropriate for investigating and explaining field closure in mathematical terms. Furthermore, we confine attention to the inner side of the unperturbed separatrix, avoiding the need for non-Solov'ev boundary conditions. Field closure under odd-parity perturbations was previously reported in FRCs by three other techniques, field-line tracing, graphical,[4] and MHD.[9]

Again, we chose the Solov'ev equilibrium[10] because of its mathematical tractability. In cylindrical co-ordinates, the FRC magnetic field inside the separatrix is described by

$$(B_r, B_\phi, B_z) = B_0\left(\frac{rz}{z_s^2}, 0, 1 - \frac{2r^2}{r_s^2} - \frac{z^2}{z_s^2}\right), \tag{1}$$

where B_0 is the magnitude of the FRC field at $z = r = 0$. r_s and z_s are the semi-minor and semi-major axes of the separatrix of the unperturbed Solov'ev field, respectively. The field is independent of ϕ and, hence, can be summarized by a scalar flux function ψ. Using the flux function, the magnetic field can be written as $(B_r, B_z) = (-(1/r)\partial_z\psi, (1/r)\partial_r\psi)$ or $\mathbf{B} = \nabla\psi \times \hat{\phi}/r$. The contours of constant ψ are perpendicular to its gradient. $\mathbf{B}$ is also perpendicular to $\nabla\psi$ and on the same plane; hence, $\mathbf{B}$ is tangent to the contours of ψ.

For the Solov'ev FRC, the ψ is

$$\psi = \frac{B_0}{2}r^2\left(1 - \frac{r^2}{r_s^2} - \frac{z^2}{z_s^2}\right). \tag{2}$$

For perturbed field lines, the magnetic field is not independent of ϕ. The flux function concept cannot be applied to analyze the field lines. Our goal is to formulate a specific type of flux function for the FRC, including perturbations cases.

A general class of anti-symmetric perturbations can be expressed by the following equations:[11]

$$\Delta B_r = -2\alpha B_0\left(I_0(kr) - \frac{I_1(kr)}{kr}\right)\sin kz \cos\phi, \tag{3a}$$

$$\Delta B_\phi = 2\alpha B_0\frac{I_1(kr)}{kr}\sin kz \sin\phi, \tag{3b}$$

$$\Delta B_z = -2\alpha B_0 I_1(kr)\cos kz \cos\phi, \tag{3c}$$

where α represents a ratio factor of the perturbation field strength to the FRC field strength, B_0. I_0 and I_1 are the modified Bessel functions of the first kind.

We begin by assuming α small and that $kz, kr \ll 1$. We will later extend α to larger values to understand phase transitions. Regardless of the assumption on α, this approximates—to second order in kz_s and kr_s—the odd-parity perturbation as

$$\Delta\mathbf{B} \approx -\alpha B_0(kz\cos\phi, -kz\sin\phi, kr\cos\phi). \tag{4}$$

The earlier work[4] assumed $kr_s \ll 1$, though not necessarily $kz_s \ll 1$. The closure of the field lines happens in the neighborhood of equilibrium points, located in the plane $z = 0$. In the neighborhood of the equilibrium points, $z \to 0$ leads to $\sin kz \to kz$, $\cos kz \to 1$, e.g., Eq. (4). Hence, the closure analysis around the equilibria on $z = 0$ axis is accurate as long as $kr_s \ll 1$. Analysis of the shape will require small kz_s as well. This analysis will show that, within a specific range of α, the field lines retain their closed structure around a radially shifted equilibrium, in sharp contrast to even-parity perturbations which, even of arbitrary smallness, destroy closed-ness.[2] We will also analyze which value of α opens up the field lines and the behavior after that transition.

By the method described below, quantitative information about the change in the shape of the field structure is extracted. These results are valid strictly for perturbations with a long wavelength, namely, $kr_s, kz_s \ll 1$. As we will see, the shape of the field structure goes through a sharp transition after α crosses a critical limit.

III. CONSTRUCTION OF MODIFIED FLUX FUNCTION

We begin with the two-dimensional case, on the y–z plane at $\phi = 0$, using Cartesian co-ordinates. Adding an odd-parity perturbation, Eq. (4), to the FRC field gives the projection of the field lines onto the y–z plane as

$$B_y = B_0\frac{yz}{z_s^2} - \alpha B_0 kz, \tag{5a}$$

$$B_z = B_0\left(1 - \frac{2y^2}{r_s^2} - \frac{z^2}{z_s^2}\right) - \alpha B_0 ky. \tag{5b}$$

Normalizing by B_0, the parametric field equations become

$$\frac{dy}{dt} = \frac{yz}{z_s^2} - \alpha kz, \tag{6a}$$

$$\frac{dz}{dt} = \left(1 - \frac{2y^2}{r_s^2} - \frac{z^2}{z_s^2}\right) - \alpha ky. \tag{6b}$$

Only the parametric relationship between y and z is required; hence, t may be eliminated. Scaling by $1/z$ changes each vector's length and not its direction; the new vectors remain tangent to the field line. In other words, we are now expressing r and z in terms of $s = \int z\,dt$. Defining $S = z_s^{-2}\int z\,dt$, $Y = y/r_s$, $Z = z/z_s$, $A = \alpha kz_s^2/r_s$, and $m = r_s/z_s$ provides the dimensionless form of Eqs. (6), the new field lines

$$\frac{dY}{dS} = Y - A, \tag{7a}$$

$$Z\frac{dZ}{dS} = (1 - 2Y^2 - Z^2) - Am^2Y. \tag{7b}$$

The solution of Eq. (7a) is

$$Y = Ce^S + A. \tag{8}$$

Replacing Y in Eq. (7b) gives

$$Z\frac{dZ}{dS} = (1 - 2A^2 - m^2A^2) - Z^2 - A(4 + m^2)Ce^S - 2C^2e^{2S}. \tag{9}$$

Defining $I = (1 - 2A^2 - m^2A^2)$ and $M = Z^2 - I$ rewrites Eq. (9) as

$$\frac{1}{2}\frac{dM}{dS} + M = -(4 + m^2)ACe^S - 2C^2e^{2S}.$$

Using superposition of particular and homogeneous solution yields

$$M = -\Psi/(C^2 e^{2S}) - \frac{2}{3}(4 + m^2)ACe^S - C^2e^{2S},$$

where Ψ is an arbitrary constant. Replacing M with $Z^2 - I$ and $C^2 e^{2s}$ with Y–A gives

$$\Psi = (Y - A)^2\left(I - Z^2 - (Y - A)^2 - \frac{2A(4 + m^2)(Y - A)}{3}\right).$$

After some algebra, we write the flux function as $\Psi = (Y - A)^2(J - (Y + A(1 + m^2)/3)^2 - Z^2)$, where

$$J \equiv 1 - \frac{\alpha^2 k^2 r_s^2}{9}\left(\frac{z_s^2}{r_s^2} + 1\right)\left(\frac{2z_s^2}{r_s^2} - 1\right). \quad (10)$$

The flux function is then scaled for dimensional constants, inserting $B_0 r_s^2/2$, and finally rewritten in the dimensioned form $\psi = B_0 r_s^2 \Psi/2$:

$$\psi = \frac{B_0}{2}(y - \alpha k z_s^2)^2\left(J - \left(\frac{y + \alpha k(z_s^2 + r_s^2)/3}{r_s}\right)^2 - \left(\frac{z}{z_s}\right)^2\right) \quad (11)$$

is called the "modified flux function" (MFF). This is not an actual magnetic flux through a surface as the previously defined flux function. The MFF is a mathematical construct whose contours describe the projection of the field lines onto y–z plane. As we will see in Sec. IV, the modification gives us important physical results. The validity of the modification is demonstrated in Fig. 1. Note that for $\alpha = 0$ or $k = 0$, the MFF reduces to the previously defined flux function equation projected to y–z plane.

IV. CLOSURE AND SHAPE OF CONTOURS OF MODIFIED FLUX FUNCTION

The modified flux function provides quantitative results for field structure geometry changes. First, we find the two-dimensional gradient of MFF, $\nabla\psi = (\psi_y, \psi_z)$. We could have simply calculated the gradient and Hessian of the unperturbed function to understand stability of the system. However, we want to extract more information than just qualitative statements on the stability of the system, such as when the system becomes unstable, what are the new critical-point locations, and if there are other critical points hidden in the system. For these, a cumbersome calculation of the gradient and Hessian of perturbed field is necessary. After doing the necessary calculations, we find that

$$\psi_y = B_0(y - \alpha k z_s^2)\left(1 - \frac{2y^2}{r_s^2} - \frac{z^2}{z_s^2} - \alpha k y\right) = B_z(y - \alpha k z_s^2), \quad (12a)$$

$$\psi_z = -B_0(y - \alpha k z_s^2)^2\frac{z}{z_s^2} = -B_y(y - \alpha k z_s^2). \quad (12b)$$

Setting the gradient to 0 gives the critical points. An easy-to-spot solution is $y = \alpha k z_s^2$. This means that the critical points of the first type lie on the line $(y, z) = (y_0, z)$, where we defined

$$y_0 = \alpha k z_s^2.$$
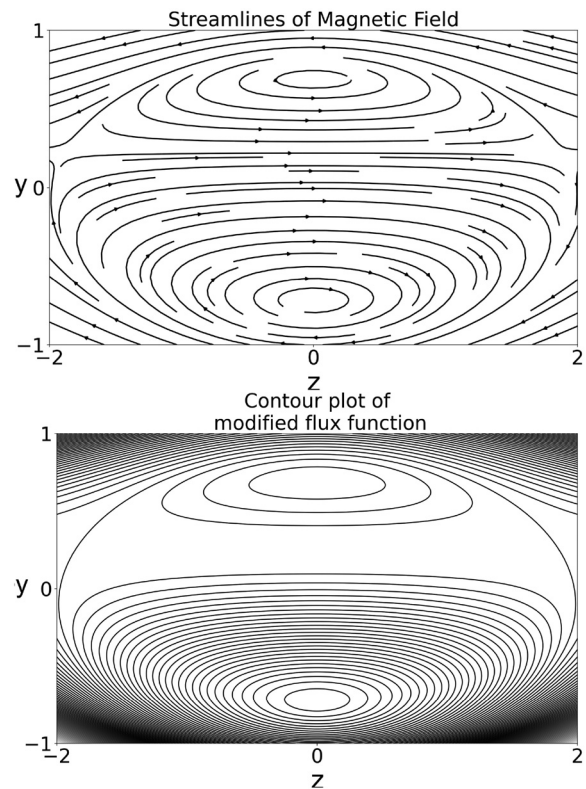
FIG. 1. Verification that the modified flux function aligns with projection of field lines on y–z plane. In the top figure, exact perturbation from Eq. (3) was used to plot the field lines. The lower figure plots MFF derived from the approximated perturbation from Eq. (4). They result in the same closed curves. One half of FRC expands, while the other half contracts. The separatrix shifts in the direction where the contours expand. Here, $r_s = 1$, $z_s = 2$, $B_0 = 1$, $\alpha = 0.2$, and $k = 0.3$.

The other solution where $y \neq \alpha k z_s^2$ requires $\psi_z = 0$ and thus $z = 0$. Using $z = 0$ on $\psi_y = 0$ with the condition $y \neq \alpha k z_s^2$ requires

$$1 - \alpha k y - 2\left(\frac{y}{r_s}\right)^2 = 0.$$

Solving this gives two possible values for y and the two isolated critical points of second type $(y_\pm, 0)$. $y_\pm$ is found by solving the stated quadratic equation and is given as follows:

$$y_\pm = -\frac{\alpha k r_s^2}{4} \pm r_s\sqrt{\frac{1}{2} + \frac{\alpha^2 k^2 r_s^2}{16}}. \quad (13)$$

To understand the nature of these critical points, we have to find the determinant of the Hessian matrix of the MFF. The Hessian matrix is given by

$$H_\psi(y, z) = \begin{pmatrix} \psi_{yy} & \psi_{yz} \\ \psi_{zy} & \psi_{zz} \end{pmatrix}.$$

The trace of the Hessian matrix is $Tr[H_\psi] = \psi_{yy} + \psi_{zz}$ and the determinant of the Hessian matrix is $\det[H_\psi] = \psi_{yy}\psi_{zz} - \psi_{yz}^2$. After the necessary calculations, we find their closed forms
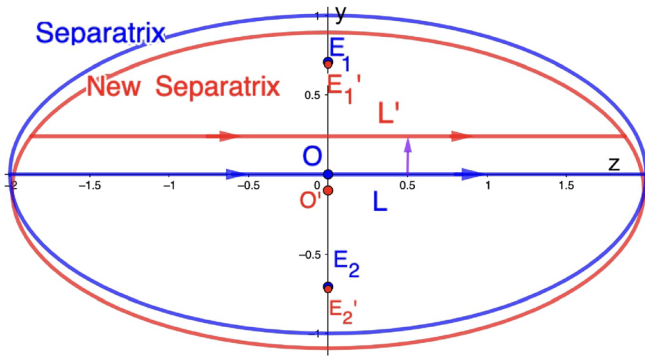
FIG. 2. Schematic of the separatrices (ellipses), separator lines, and ellipse centers before and after application of the perturbation. The perturbation causes the separatrix center to go down to O' from O, but the separator line to go up to L' from L. The separator and separatrix are part of the same level curve $\psi = 0$. The equilibrium points, E_1 and E_2, move down to E_1' and E_2'. $r_s = 1$, $z_s = 2$, $\alpha = 0.2$, and $k = 0.3$.

$$Tr\left[H_\psi(y,z)\right] = B_0\left(1 - \frac{z^2}{z_s^2} + \frac{4\alpha k z_s^2 y}{r_s^2} - \frac{y^2}{z_s^2} - \frac{6y^2}{r_s^2}\right), \quad (14)$$

$$\det\left[H_\psi(y,z)\right] = -\frac{B_0^2}{z_s^2}(y - \alpha k z_s^2)^2 D(y,z), \quad (15a)$$

$$D(y,z) \equiv 1 + \alpha^2 k^2 z_s^2 + \frac{3z^2}{z_s^2} - \frac{6y^2}{r_s^2} + 2\alpha k y\left(\frac{2z_s^2}{r_s^2} - 1\right). \quad (15b)$$

It is easy to see that the critical points on the line $(y,z) = (\alpha k z_s^2, z)$ have $\det[H_\psi] = 0$ (Fig. 2). So, the Hessian is a semi-definite, and all critical points of the first type are degenerate critical points.[12] They form a critical manifold, which we define as the separator line.[12] In general, the critical manifolds are unstable when perturbed and turn into a sequence of isolated critical points. However, as we see here, the gradient and Hessian remain 0 on the separator line regardless of α of the perturbation. So, as the critical manifold, or as we defined it, the separator line is stable under odd perturbation. The critical points of second type have $\det[H_\psi] \neq 0$. If $D(y,z) > 0$, then $\det[H_\psi] < 0$ and, thus, the point is a saddle point. If $D(y,z) < 0$, then $\det[H_\psi] > 0$ and the point is a local maximum/minimum. If it is local maximum, then the Hessian has a negative trace; otherwise, it has a positive trace. Given its importance, we label the quantity as $D(y,z)$ characterizer.

We should note now that we are going to use the word "critical points of the first type," "points from separator line," and "degenerate critical points" interchangeably. We will also use "critical points of the second type" and "isolated critical points" interchangeably.

We summarize the discussion in the following table (Table I). The following table is true for the critical points of the second type.

TABLE I. Classification of minima and maxima: Critical points of the second type.

Characterizer	Trace	Classification	Closure
$D < 0$	$Tr < 0$	Local maxima	Yes
$D < 0$	$Tr > 0$	Local minima	Yes
$D > 0$	Any value	Saddle point	No
$D = 0$	Any value	Degenerate point	Uncertain

The trace of the Hessian and characterizer of the critical points of the second type are

$$Tr\left[H_\psi(y_\pm, 0)\right] = -2B_0\left(1 + \frac{r_s^2}{4z_s^2}\right)$$
$$\times \left(1 + \alpha k\left(r_s + \frac{2z_s^2}{r_s}\right)\left(\frac{\alpha k r_s}{4} \mp \sqrt{\frac{1}{2} + \frac{\alpha^2 k^2 r_s^2}{16}}\right)\right), \quad (16)$$

$$D(y_\pm, 0) = -4\left(\frac{1}{2} + \frac{\alpha^2 k^2 r_s^2}{16}\right) \pm \alpha k\left(r_s + \frac{4z_s^2}{r_s}\right)\sqrt{\frac{1}{2} + \frac{\alpha^2 k^2 r_s^2}{16}}. \quad (17)$$

For arbitrary $\alpha > 0$, $D(y_-, 0) < 0$ and $Tr[H_\psi(y_-, 0)] < 0$. So, the lower critical point of second type is always a local maxima. In addition, for small enough α, $D(y_+, 0) < 0$ and $Tr[H_\psi(y_+, 0)] < 0$ are also true. So, for small enough α, both critical points of second type are local maxima. Hence, the immediate contours near the critical points of the second type are closed.[12] Similar results have been found in the context of tokamak equilibria in the presence of current reversal.[13] We can go further and prove the following two theorems (the proofs of these theorems can be found in Appendix C).

Theorem 1: All contours, except the separator line, within the ellipse from Eq. (18) are closed,

$$\left(\frac{y + \alpha k(z_s^2 + r_s^2)/3}{r_s}\right)^2 + \left(\frac{z}{z_s}\right)^2 = J. \quad (18)$$

Theorem 2: For small enough α, such that two local maxima exists inside the ellipse in Eq. (18), all contours outside the ellipse are open.

Using these two theorems, we can define our separatrix as the ellipse described in Eq. (18). Separatrix separates the closed field lines from the open field lines. It should be noted that these theorems only work if the two isolated critical points are within the ellipse. If they are outside, the situation is different, and we have a different separatrix.

We can find the length of the separator line contained within the ellipse by finding the distance of intersection points. As the separator line is $(y, z) = (\alpha k z_s^2, z)$, we can set $y = \alpha k z_s^2$ in Eq. (18) and then solve for z to find the intersection points. Given that they have same $y = \alpha k z_s^2$ and symmetric with respect to $z = 0$ axis, we can just multiply the value of z to find the length of the segment. It comes out as

$$l = 2z_s\sqrt{1 - \alpha^2 k^2 z_s^2\left(\frac{2z_s^2}{r_s^2} + 1\right)}. \quad (19)$$

We now summarize our key findings of field structure for small α:

1. The separator line separates the upper half of the closed field lines and the lower half of the closed field line. It lies on the z-axis in the unperturbed case. When a perturbation is added, it shifts from $y = 0$ to $y = \alpha k z_s^2$. The flatter sections of the field lines, those closer to the z-axis, shift more. This separator line is stable under odd perturbation.

2. The separatrix retains nearly the same elliptical shape with the same semi-minor and semi-major axis ratio. The area enclosed

by the separatrix is scaled by $J \approx 1 + \mathcal{O}(\alpha^2 k^2)$, second order with respect to α and k.

3. The separator line segment, demarcated by the separatrix, has length $2z_s\sqrt{1 - \alpha^2 k^2 z_s^2 (2z_s^2/r_s^2 + 1)}$.

4. Information about the positions of the new stable equilibrium points, E_1' and E_2', can be derived from solving $\mathbf{B} = 0$ near the unperturbed equilibria in y–z plane. Setting $\mathbf{B} = 0$ in Eq. (6) gives us $z = 0$ and $y_\pm = -\alpha k r_s^2/4 \pm r_s\sqrt{1/2 + \alpha^2 k^2 r_s^2/16}$ $\approx \pm r_s/\sqrt{2} - \alpha k r_s^2/4 + \mathcal{O}(\alpha^2 k^2)$. As expected, the equilibrium points are same as local maxima derived from Eq. (13). The equilibrium points move down by $\sim\alpha k r_s^2/4$.

V. OPENING OF MAGNETIC FIELD LINES: A DISCONTINUITY

For large enough α, the field topology changes drastically. The analysis of field topology needs to be updated for such a case. This change may be analyzed by focusing on the upper isolated non-degenerate point $(y_+, 0)$. As α increases, at a critical value α_*, the upper local maximum at $(y_+, 0)$ becomes a saddle point. This happens when the characterizer starts to become negative. The critical α_* can be estimated by setting the characterizer, $D(y_+, 0) = 0$. $D(y_+, 0)$ is calculated from Eq. (17),

$$-4\left(\frac{1}{2} + \frac{\alpha_*^2 k^2 r_s^2}{16}\right) + \alpha_* k\left(r_s + \frac{4z_s^2}{r_s}\right)\sqrt{\frac{1}{2} + \frac{\alpha_*^2 k^2 r_s^2}{16}} = 0.$$

Solving for α_* gives

$$\alpha_* = \frac{1}{kz_s\sqrt{1 + \frac{2z_s^2}{r_s^2}}}, \tag{20}$$

where α_* is also the critical value for two other important transitions. First, α_* is the value for which the separator line starts to move outside of the ellipse (see Lemma 3, Appendix B). Second, at $\alpha = \alpha_*$, the upper isolated critical point $(y_+, 0)$ starts to move outside of the ellipse from Eq. (18) (see Lemma 4, Appendix B).

Given that two local maxima are no longer inside the ellipse, Theorem 2 no longer represents the system and does not help to evaluate the separatrix. The separatrix covers a larger region than what would be predicted by the ellipse. Given the new situation, we have a new separatrix, given by the Theorem 3. The detailed proof of Theorem 3 is outlined in Appendix C.

Theorem 3: For $\alpha > \alpha_*$, all contours inside $\psi(y, z) = \psi(y_+, 0)$ are closed and all contours outside of it are open.

This means no contour is closed besides ones obeying $\psi > \psi(y_+, 0)$. So, the new separatrix is $\psi(y, z) = \psi(y_+, 0)$. This curve itself is not closed, but all closed curves are part of an open set with this new curve as the boundary. The new separatrix is no longer smooth everywhere, specifically at the point $(y_+, 0)$. This transition is abrupt, modifying the separatrix equation to

$$\psi(y, z) = \begin{cases} 0 & \text{when } \alpha < \alpha_*, \\ \psi(y_+, 0) & \text{when } \alpha > \alpha_*. \end{cases} \tag{21}$$

As demonstrated in detail in Sec. IV, prior to the transition, the separatrix is a smooth ellipse. At the transition, the separatrix

TABLE II. Effect of phase transition on important features of field lines: local maxima/minima, saddle points, and region of closed field lines.

Ratio factor α	Local maxima	Saddle points	Region of closure
$\alpha < \alpha_*$	$(y_\pm, 0)$	None	$\psi(y, z) > 0$
$\alpha > \alpha_*$	$(y_-, 0)$	$(y_+, 0)$	$\psi(y, z) > \psi(y_+, 0)$

develops a corner (Fig. 3). The phase transition is summarized in Table II.

To check the theoretical derivation, a numerical analysis was performed using the exact perturbed field from Eq. (3) with $k = 0.3$, $r_s = 1$, and $z_s = 2$. Given that we have used exact equations from the perturbed field, there is no approximation in the result from numerical analysis. As seen by closely inspecting the streamlines of the non-approximated perturbed field, beyond $\alpha_{,*} = 0.54761$, the field lines open at the first equilibrium point in the $\phi = 0$ plane. Bifurcation of the evolving field topology is clear as variations as small as $\sim 10^{-5}$ around $\alpha = 0.54761$ in the region $y \in [-0.66702, 0.66704]$ and $z \in [-0.01, 0.01]$ demonstrate (see Fig. 4). For $r_s = 1$, $z_s = 2$, $k = 0.3$, Eq. (20) gives $\alpha_* = 0.5556$, close to the numerical result. Most of the difference arises from the approximation made for the perturbation field's dependence on r.

VI. LIMITATIONS OF THIS METHOD

MFF analysis has been able to explain most of the numerically observed results quantitatively. However, the Solov'ev FRC with specified perturbations is an approximate system. For high values of wavenumber k, the theoretical prediction from the approximation made in Eq. (4) starts to break down. The disagreements are not just quantitative; there are qualitative changes in field structure that our theory fails to grasp. Within a certain range of α, two nodes form, toward or from which all field lines spiral. Numerical calculations were made using the
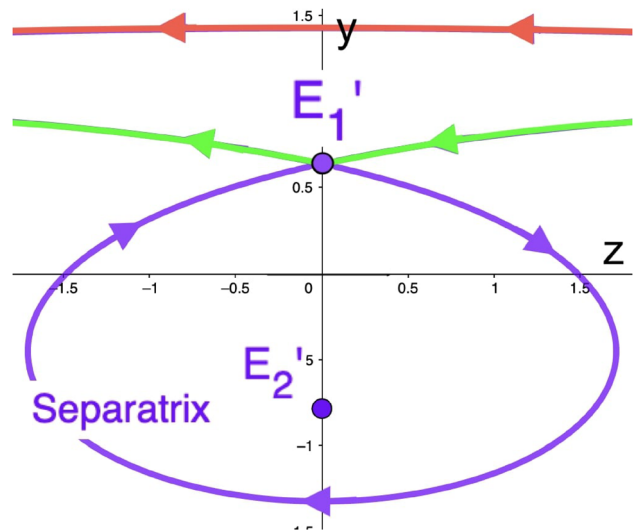
FIG. 3. For $\alpha > \alpha_*$, the separatrix (denoted by purple) develops an x point, E_1'. The lines above the x-point (orange and green) are not part of the separatrix but are on same level set. The critical point E_1' is now a saddle point, while E_2' remains a local maximum.
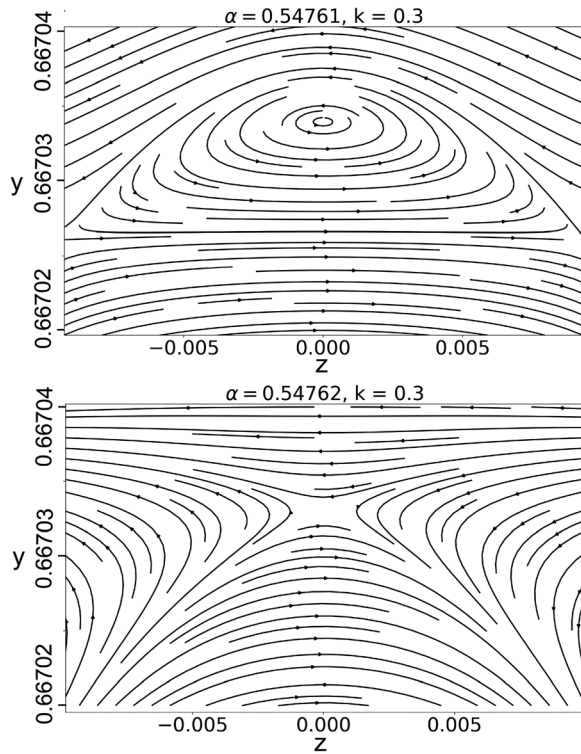
FIG. 4. The field lines near the first equilibrium point for two closely spaced perturbation strengths. Top figure, $\alpha = 0.547\,61$, closed structure; lower figure, $\alpha = 0.574\,62$, open structure. The field lines are calculated using one exact odd-parity perturbation and projected on y–z plane. $r_s = 1$, $z_s = 2$, $k = 0.3$.

exact perturbation, Eq. (3), with a high value for the wave-number k, something our approximated system assumed to be small. A system with $r_s = 1$, $z_s = 2$, $k = 1$ displays this phenomenon for $0.143 < \alpha < 0.162$. This structure begins when k exceeds a critical value, $k_* \approx 0.8$. The nodes are not on $z = 0$, and thus, the approximation of $\sin kz \rightarrow kz$, $\cos kz \rightarrow 1$ is not valid in describing them unless the wave-number k is small; information about the exact nature of closure on points outside that area cannot be extracted. Some results are displayed in Fig. 5. Analyzing these results requires a complete solution of the perturbation equations which uses the exact perturbation [Eq. (3)]. In the future, we would like to find the exact solution or add additional terms from the Taylor series approximation and try to find an analytical approach to this phenomenon.

VII. GENERALIZATION OF THE MODIFIED FLUX FUNCTION TO 3D SPACE

The three-dimensional perturbation in Eq. (4) can be solved in a similar way. In Cartesian co-ordinates, the perturbation is written as $\Delta \mathbf{B} = \alpha B_0(0, kz, ky)$ and the FRC magnetic field is $\mathbf{B} = -B_0(xz/z_s^2, yz/z_s^2, 1 - 2(x^2/r_s^2 + y^2/r_s^2) - z^2/z_s^2)$. Following Eqs. (7a)–(11) provides

$$\frac{dX}{ds} = X; \quad \frac{dY}{ds} = Y - A; \quad Z\frac{dZ}{ds} = 1 - 2(X^2 + Y^2) - Z^2 - Am^2Y,$$

$$(22)$$
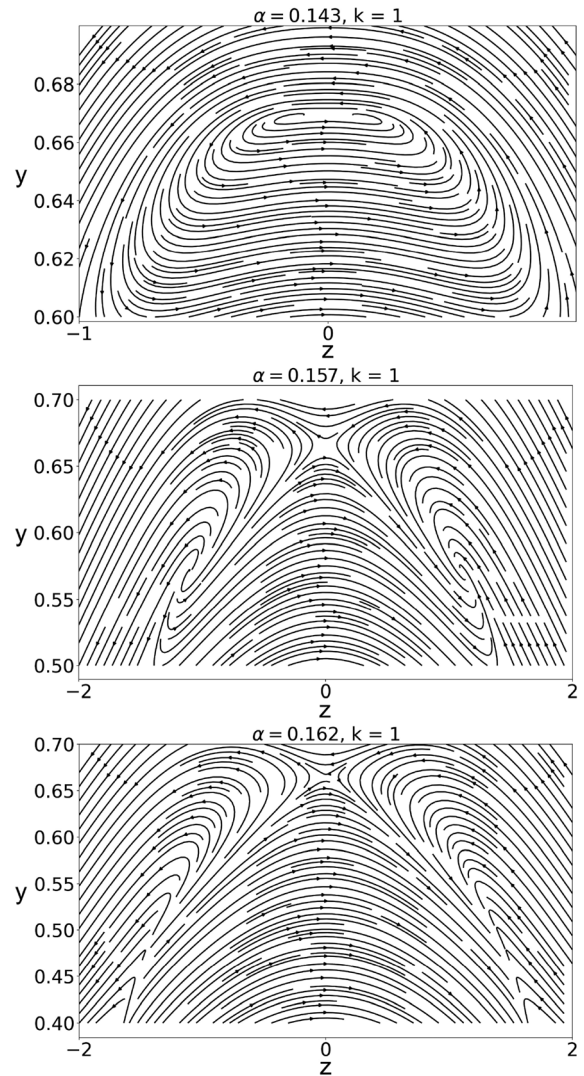
FIG. 5. Formation of two nodes. When α is within 0.143 and 0.163, field lines spiral toward or from these nodes. Here, $k = 1$, $r_s = 1$, $z_s = 2$, and this is projection of field lines on y–z plane. Odd-parity perturbation [Eq. (3)]. This effect was only observed for $k \approx 0.8$ or higher.

which can be solved using the same methods as in Sec. III. Some of the features of the result and the nature of the magnetic field lines are

1. In the approximation of small k, the field lines remain in the same plane, which goes through line $(0, \alpha k z_s^2, z)$ and makes slope (arbitrary constant, c) with the x-axis, meaning x and y of a field line follow the relationship

$$y = cx + \alpha k z_s^2. \qquad (23)$$

Large k causes the surface to warp, as shown in Fig. 8 of Ref. 4.

2. The field lines stay closed and remain on level sets of the MFF, with ψ defined in Eq. (2) and J defined as before,

$$\psi = \frac{B_0}{2}\mathbf{u}^2(J - \mathbf{v}^2),$$

$$\mathbf{u} = (x, y - \alpha k z_s^2, 0),$$

$$\mathbf{v} = \left(\frac{x}{r_s}, \frac{y + \alpha k(z_s^2 + r_s^2)/3}{r_s}, \frac{z}{z_s}\right).$$

3. The field lines are intersections of planes of Eq. (23) and the level sets of MFF, ψ. The arbitrary constants defining a singular field line are $c \in \mathbb{R}$ and $\psi \in \mathbb{R}$. The level sets of ψ are plotted in Fig. 6.

4. Again, the separator line is moved by $\alpha k z_s^2$ in the positive y direction and the center of the separatrix is moved by $\alpha k(z_s^2 + r_s^2)/3$. The separatrix remains nearly an ellipsoid with same ratio of axes. The volume enclosed by separatrix is scaled by $J^{3/2} \approx 1 + \mathcal{O}(\alpha^2 k^2)$.
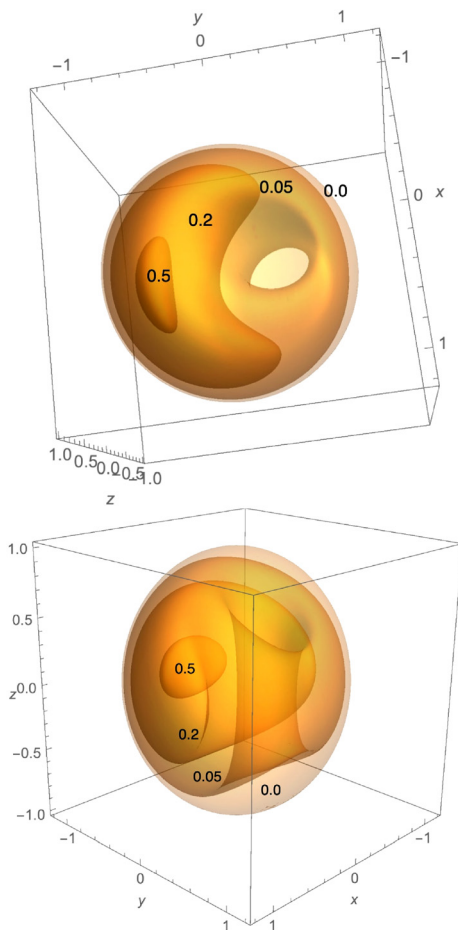
FIG. 6. Level sets of $\psi = 0.0, 0.05, 0.2,$ and 0.5 for $r_s = z_s = 1$, $\alpha = 0.5$, and $k = 0.4$. The $\psi = 0$ creates a separatrix and field lines outside of that are open. Within the separatrix, field lines lie in the intersection of level sets and $y = cx + \alpha k z_s^2$ surfaces. The top figure is a view from above and the bottom figure from the side.

VIII. DISCUSSION AND SUMMARY

We developed a mathematical tool called the modified flux function (MFF) to understand the effects of perturbations on a Solov'ev FRC field structure. We have confined attention to the inner region of the FRC, near the O-point line, avoiding the region outside the separatrix where the Solov'ev solution is not physical. For reactor-scale FRC's, though the ion s_i value may be small, <10, where $s_i \sim 0.3 r_s/\rho_i$, that for electrons is large, $s_e \sim 1000$. Electrons follow field lines, and associated particle and energy losses on open field lines would be important.

The analytical results derived from the MFF have reproduced the previous numerical observation that small odd-parity perturbation preserves FRC field structure. In particular, the contours around the equilibrium stay closed. Qualitative assertions about change in field topology, e.g., movement of the center of separatrix, separator line, and other geometric parameters, were made in the previous work.[4] MFF has provided quantitative values of these quantities. Through the use of the MFF, we identified a bifurcation of the field structure with increasing perturbation strength and its quantitative threshold.

AUTHOR DECLARATIONS
Conflict of Interest

The authors have no conflicts to disclose.

Author Contributions

Taosif Ahsan: Conceptualization (equal); Formal analysis (lead); Methodology (lead); Visualization (lead); Writing – original draft (lead). **Samuel A. Cohen:** Conceptualization (equal); Funding acquisition (lead); Methodology (supporting); Project administration (lead); Supervision (lead); Writing – review and editing (supporting).

DATA AVAILABILITY

The data that support the findings of this study are openly available in the cited website at http://arks.princeton.edu/ark:/88435/dsp01x920g025r, Ref. 14.

APPENDIX A: POINCARÉ–HOPF THEOREM

The Poincaré–Hopf theorem states, if $\mathbf{A}$ is a vector field on a compact differentiable manifold M, then[15,16]

$$\sum_i \text{index}_{x_i}(\mathbf{A}) = \chi(M). \tag{A1}$$

Here, we sum over the indices of all isolated critical points, x_i. $\chi(M)$ is the Euler characteristic.

In our case, the vector field in which we are interested is the magnetic field, **B**. The magnetic field lines are the contours of ψ. So, the magnetic fields are tangent along a closed contour of ψ. If the manifold M is enclosed by a closed contour or closed magnetic field line, ∂M, assuming there is no isolated critical point on the ∂M, we can glue two pieces of this manifold with the same vector fields together along the boundary. In this new manifold, **B** is continuous. This new manifold, M', is a closed orientable surface without any tori and thus has genus $g = 0$ with Euler characteristic $\chi(M') = 2 - 2g = 2$. Given that the vector field is the same, the critical points appear twice compared to how many times they appear in manifold M. So, in Eq. (A1), we get, $2 \sum_i \text{index}_{(y_i, z_i)}(\mathbf{B}) = 2$. Crossing out the factor two from both sides gives us

$$\sum_i \text{index}_{(y_i, z_i)}(\mathbf{B}) = 1. \tag{A2}$$

Here, the critical points are (y_i, z_i) and only summed over manifold M. So, the conclusion is that if an area is enclosed by a simple closed field line of **B**, equivalent to a simple closed contour of ψ, and critical points (y_i, z_i) of **B** are inside the area, then their indices must sum to 1. Because the contours are closed around the local maximum/minimum of ψ and magnetic field lines thus circle the critical point (once) as we follow the flow of field lines around it, the critical point of the magnetic field **B** that is a local maximum/minimum of ψ has index 1. The critical saddle points of the magnetic field **B** must be critical saddle points of ψ. So, the critical points of **B**, which are critical saddle points of ψ, must have index -1.

Subsequently, if an area enclosed by a simple closed field line of **B** (equivalent to a simple closed contour of ψ) contains $n_{\max}, n_{\min}$, and n_{saddle} which are the number of local minima, maxima, and saddles points and no degenerate points, the following must be true from Eq. (A2):

$$n_{\max} + n_{\min} - n_{saddle} = 1. \tag{A3}$$

APPENDIX B: PROOFS OF LEMMAS

Lemma 1: If a contour intersects the separator line or is tangent to it, then it can only be the ellipse described in Eq. (18).

Proof: Now we know that the line $(y, z) = (\alpha k z_s^2, z)$ contains all the degenerate critical points. If a contour intersects or is tangent to the ellipse from Eq. (18), then in that shared point, it has $\psi = 0$ due to $y - \alpha k z_s^2 = 0$ on the separator line. It is a contour and, thus, must have $\psi = 0$ on all its points. Given that it cannot be the separator line itself, the other factor in $\psi = 0$ must be equal to the ellipse from Eq. (18). Q.E.D.

Lemma 2: If an open contour intersects the ellipse described in Eq. (18) or is tangent to it, then it can only be the separator line.

Proof: If the contour intersects or is tangent to the ellipse in Eq. (18), then it must share at least one point and given that the value of ψ is 0 in that point, it must also be 0 for the contour. As the contour cannot be the ellipse from Eq. (18), $\psi = 0$ only gives us $y - \alpha k z_s^2 = 0$ or the separator line. So, the contour must be the separator line. Q.E.D.

Lemma 3: For $\alpha > \alpha_*$, the ellipse from Eq. (18) does not intersect or touch the separator line.

Proof: From Eq. (19), we can see that the length of the segment of separator line within the ellipse from Eq. (18) is $l = 2 z_s \sqrt{1 - \alpha^2 k^2 z_s^2 (2 z_s^2 / r_s^2 + 1)} = 2 z_s \sqrt{1 - \alpha^2 / \alpha_*^2}$. For $\alpha > \alpha_*$, this length is imaginary and, thus, the separator line cannot touch or intersect the ellipse as that would result in a real value for l. Q.E.D.

Lemma 4: For $\alpha > \alpha_*$, the upper isolated critical point $(y_+, 0)$ resides outside of the ellipse from Eq. (18).

Proof: We know from Eq. (20) that, for $\alpha > \alpha_*$, the upper isolated critical point is a saddle point. We also know that the ellipse from Eq. (18) is a valid closed contour with $\psi = 0$, and Lemma 3 entails that the separator line is outside of the ellipse. So, the ellipse is a valid closed contour without any degenerate critical points inside it and we can apply Eq. (A3).

Let us assume the upper isolated critical point is inside the ellipse. We have two cases:

Case 1: The lower isolated critical point, which is always a local maxima, is inside the ellipse. Then, we have $n_{\max} + n_{\min} - n_{saddle} = 1 + 0 - 1 = 0 \neq 1$.

Case 2: The lower isolated critical point is outside of the ellipse. Then, $n_{\max} + n_{\min} - n_{saddle} = 0 + 0 - 1 = -1 \neq 1$. Both cases lead to contradictions and the lemma is proven. Q.E.D.

Lemma 5: For $\alpha > \alpha_*$, the closed curve cannot contain any degenerate critical point from the separator line.

Proof: If the area inside the closed curve contained any degenerate critical points, the closed curve intersects the separator line or is tangent to it, and Lemma 1 would mean that the closed curve is the ellipse from Eq. (18). However, Lemma 3 states that for $\alpha > \alpha_*$, the ellipse does not intersect or touch the separator line. This is contradictory. Q.E.D.

APPENDIX C: PROOFS OF THEOREMS

Theorem 1: All contours, except the separator line, within the ellipse from Eq. (18) are closed.

Proof: Now, let us assume there is an open contour, which is not the separator line, inside the region enclosed by the ellipse. Given that the contour is open, it must extend to infinity in some direction and necessarily intersects the ellipse. Using Lemma 2 (see Appendix B), we can conclude that it can only be the separator line. This contradiction proves our theorem. Q.E.D.

Theorem 2: For small enough α, such that two local maxima exist inside the ellipse in Eq. (18), all contours outside the ellipse are open.

Proof: If there existed a closed contour outside of this ellipse, then there are two cases.

Case 1: The closed contour does not contain the two local maxima inside the ellipse. A closed contour without any critical point inside is impossible.[12] So, the contour contains at least one critical point outside the ellipse. Outside of the ellipse, there are only degenerate critical points on the separator line. So, the closed contour must intersect the separator line and, due to Lemma 1 (see Appendix B), can only be the ellipse which is a contradiction.

Case 2: The closed contour contains the two local maxima inside the ellipse. In this case, the contour intersects the separator, leading to the same contradiction and thus proving our theorem through contradiction. Q.E.D.

Theorem 3: For $\alpha > \alpha_*$, all contours inside $\psi(y, z) = \psi(y_+, 0)$ are closed and all contours outside of it are open.

Proof: For $\alpha > \alpha_*$, the contours that contain the local maximum $(y_-, 0)$ but do not touch the saddle point $(y_+, 0)$ are closed.[12] This means that the contours inside $\psi(y, z) = \psi(y_+, 0)$ are closed.

Let us assume that a closed contour exists outside of the $\psi(y, z) = \psi(y_+, 0)$ region. The closed contour contains the saddle point as it is outside of $\psi(y, z) = \psi(y_+, 0)$ region. However, it cannot contain any degenerate critical points from the separator line because of Lemma 5 (see Appendix B). This gives us two possible cases:

Case 1: The closed contour only contains the saddle point $(y_-, 0)$.

Case 2: The closed curve contains the saddle point $(y_+, 0)$ and local maximum $(y_-, 0)$.

Cases 1 and 2 contradict Eq. (A3). For case 1, there is one saddle point inside the closed contour. So, $n_{max} + n_{min} - n_{saddle} = 0 + 0 - 1 = -1 \neq 1$. For case 2, there is one local maximum and one saddle point inside the closed contour. So, $n_{max} + n_{min} - n_{saddle} = 0 + 1 - 1 = 0 \neq 1$. Both cases, thus, lead to contradictions. This means all contours outside of $\psi(y, z) = \psi(y_+, 0)$ must be open. Q.E.D.

REFERENCES

[1] W. N. Hugrass, I. R. Jones, K. F. McKenna, M. G. R. Phillips, R. G. Storer, and H. Tuczek, "Compact torus configuration generated by a rotating magnetic field: The rotamak," Phys. Rev. Lett. **44**, 1676–1679 (1980).

[2] A. H. Boozer, Nucl. Fusion **18**, 1663 (1978).

[3] S. W. H. Cowley, "A qualitative study of the reconnection between the Earth's magnetic field and an interplanetary field of arbitrary orientation," Radio Sci. **8**(11), 903–913, https://doi.org/10.1029/RS008i011p00903 (1973).

[4] S. A. Cohen and R. D. Milroy, "Maintaining the closed magnetic-field-line topology of a field-reversed configuration with the addition of static transverse magnetic fields," Phys. Plasmas **7**(6), 2539–2545 (2000).

[5] L. C. Steinhauer, "Review of field reversed configurations," Phys. Plasmas **18**, 070501 (2011).

[6] D. C. Barnes, "Profile consistency of an elongated field-reversed configuration. I. Asymptotic theory," Phys. Plasmas **8**(11), 4856 (2001).

[7] R. L. Spencer and D. W. Hewett, "Free boundary field-reversed configuration (FRC) equilibria in a conducting cylinder," Phys. Fluids **25**, 1365 (1982).

[8] C. P. S. Swanson and S. A. Cohen, "The effect of rigid electron rotation on the Grad–Shafranov equilibria of a class of FRC devices," Nucl. Fusion **2**, 1947–1969 (2021).

[9] R. D. Milroy, C. C. Kim, and C. R. Sovinec, "Extended magnetohydrodynamic simulations of field reversed configuration formation and sustainment with rotating magnetic field current drive," Phys. Plasmas **17**, 062502 (2010).

[10] L. S. Soloviev, Sov. Phys. JETP **26**, 400 (1968).

[11] A. H. Glasser and S. A. Cohen, "Ion and electron acceleration in the field-reversed configuration with an odd-parity rotating magnetic field," Phys. Plasmas **9**(5), 2093–2102 (2002).

[12] V. I. Arnold, S. M. Gusein-Zade, and A. N. Varchenko, *Singularities of Differentiable Maps* (Birkhäuser, Boston, 1985).

[13] P. Rodrigues and J. P. S. Bizarro, "Topology of tokamak plasma equilibria with toroidal current reversal," Phys. Plasmas **19**(1), 012504 (2012).

[14] See http://arks.princeton.edu/ark:/88435/dsp01x920g025r for the graphic.

[15] H. Poincaré, "On curves defined by differential equations," J. Math. Pures. Appl. **3**, 251 (1882).

[16] H. Hopf, "Ausbildungsklassen.*n*-dimensionaler Mannigfaltigkeiten," Math. Ann. **96**, 209–224 (1927).